Eleventh East Asia-Pacific Conference on Structural Engineering & Construction (EASEC-11)
"Building a Sustainable Environment"
November 19-21, 2008, Taipei, TAIWAN

EXPERIMENTAL RESEARCH ON HYSTERETIC PROPERTY OF UNSTIFFENED TUBULAR X-JOINTS UNDER QUASI-STATIC OUT-OF-PLANE BENDING

Xiande Meng[1], Yiyi Chen[2], Wei Wang[3], and Bida Zhao[1]

ABSTRACT : Unstiffened tubular X-joints with different geometrical parameters were experimentally researched under cyclic quasi-static out-of-plane bending, in order to investigate the seismic behavior of the joint in spacial tubular structure. In this paper, the experimental scheme is introduced. A special constraint device to release the end rotation of test specimen is described. Two failure modes occurred in the experiment, including the chord tube wall punching and brace tube wall buckling. By proper set of geometrical parameters and qualified welds, the plastic bending capacity of brace can be acquired. The results show that specimens with the smaller ratio γ of chord radius to its thickness tend to be punching of chord tube wall, instead of chord tube wall plasticizing, and that specimens with the larger ratio β of brace diameter to chord diameter behave excellent in deformability and energy-dissipation capability, the other worse in this regard.

KEYWORDS: Steel tube, X-joint, Unstiffened tubular joint, Hysteretic behavior, Experimental research

1. INTRODUCTION

In tubular truss, lattice grid and reticulated shell structures, steel hollow section members are commonly connected with unstiffened joint. The characters of joints in different structures are not identical, relating to different structural behaviors and loading transmitting mechanism. For the hysteretic properties of the unstifferned tubular joint, the research achievement having been acquired are limited in truss joint, planar or spacial, ordinary or vierendeel truss, for example planar K-joint subjected to axial forces [1], T-joint subjected to axial force and combined moment [2], spacial gap and overlap KK-joint subjected to axial force [3].

To large span roof structures, lattice grid and reticulated shell are the common structural system widely used. In seismic design, the vertical component of ground motion shall be predominant usually. Therefore unstiffened tubular joint in these structures is subjected to both axial force and bending moment in and out-of-plane of member axes. And the cyclic moments shall play main role in the failure mode and energy consumption of the joint.

Recently unstiffened tubular X-joints with different geometrical parameters were experimentally researched under cyclic quasi-static out-of-plane bending, in order to provide a base for further study on seismic resistances of spacial tubular structure.

2. TEST SPECIMENS

Three specimens were designed and fabricated, the configuration of which is shown in Figure 1, and more details of which can be found in Table 1. In the table, the nondimensional parameters are β

[1] *PH.D Candidate, College of Civil Engineering, Tongji University, Shanghai 200092, China.*
[2] *Professor, Key State Lab for Disaster Prevention in Civil Engineering, Tongji University.*
[3] *Lecturer, College of Civil Engineering, Tongji University.*

(=d/D), γ(=$D/2T$),and τ(=t/T). Both the chord and the brace were fabricated from hot-rolled tube of Q345B. And the material properties of the connections are presented in Table 2. The difference between XBH-1 and XBH-2 is the parameter β, and the difference between XBH-1 and XBH-3 is τ.

Table 1 Size of specimens

Specimen ID	$D \times T$	$d \times t$	β	γ	τ	θ	φ
XBH-1	273x16	245x12	0.90	8.53	0.75	90°	180°
XBH-2	273x16	194x12	0.71	8.53	0.75	90°	180°
XBH-3	273x16	245x7	0.90	8.53	0.44	90°	180°

Table 2 Measured material properties(average value)

Section ($D \times T$)	Yield Stress f_y (MPa)	Ultimate Stress f_u (MPa)	Elongation δ (%)	Elastic Modulus E (MPa)
273×16	368	520	30.0	2.18×10^5
245×12	385	551	30.1	2.30×10^5
194×12	358	518	24.2	2.09×10^5
245×7	398	559	26.1	2.03×10^5

3. TEST SETUP AND LOADING SCHEME

The test setup was designed to accommodate specimens with braces in a horizontal position, as shown in Figure 2. The specimen at both ends of chord was fixed on two support columns which were anchored to the floor. The load was applied to each cantilever brace end by a hydraulic actuator, through a connecting plate bolted to the brace end plate. And the hydraulic actuators were fixed on the floor, of which the loading direction is vertical to the plane of chord and brace axes.

The support column clamped the end plate of chord through upper and under coverer plates. The contact surfaces of cover plates and end plate were made of curved surfaces, which allowed the end plate to rotate around its own axis, and which resulted to achieve pinned boundary conditions.

The two actuators applied cyclic load synchronously, based on the initial position, which means that the bending curve of braces is reverse to the bending curve of chord. The test was conducted using the brace end displacement (Δ) control, mixed with loading control, as shown in Figure 3.

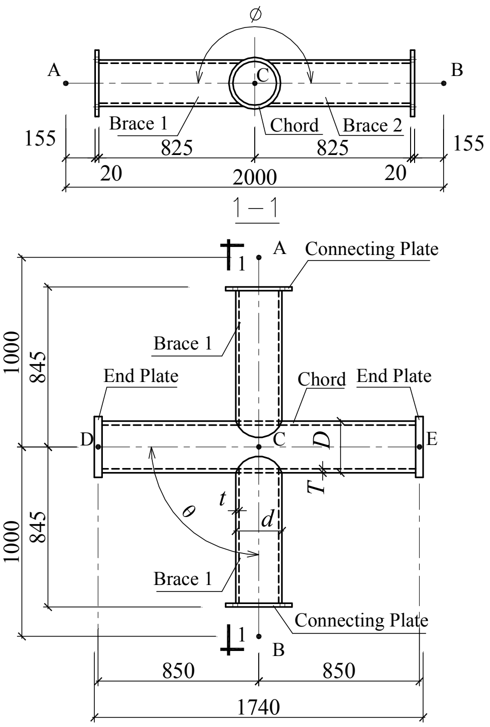

Figure 1. Test specimens

4. DATA PROCESSING

Figure 5 shows the model representing half of the specimen cut along the plane of geometrical symmetry. The diagram was characterized by the following parameters: applied load P, the brace end displacement δ (relative to the center C).

The brace end displacement δ is composed of the displacement δ_1 caused by the joint rotation θ, and the flexural deformation δ_2 of the brace itself, as shown in Figure 6. So the joint rotation θ can be given out by Equation 1.

$$\theta = \delta_1 / L_b = (\delta - \delta_2) / L_b \quad (1)$$

Where L_b is distance between crown point and loading point.

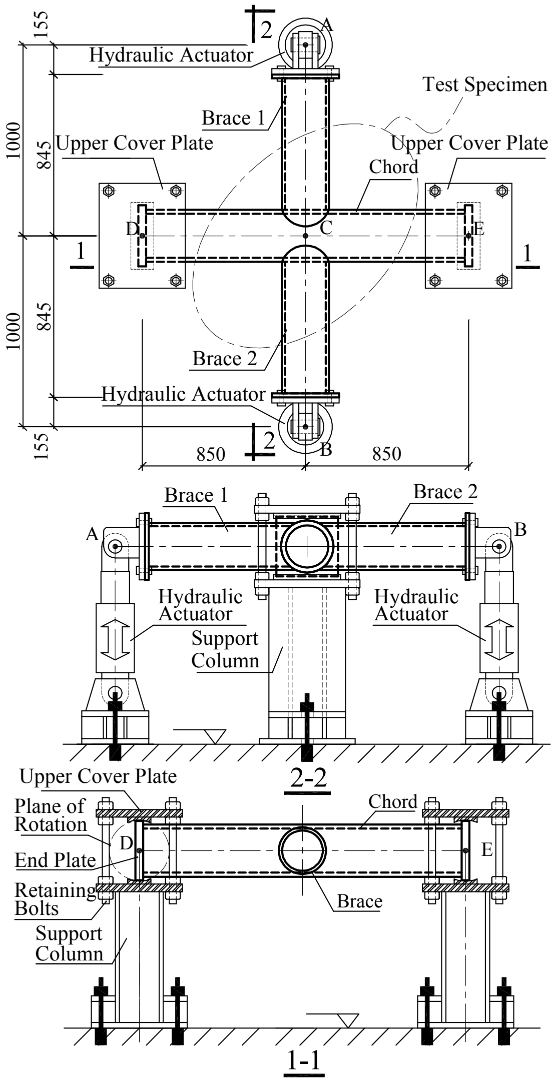

Figure 2. Test setup

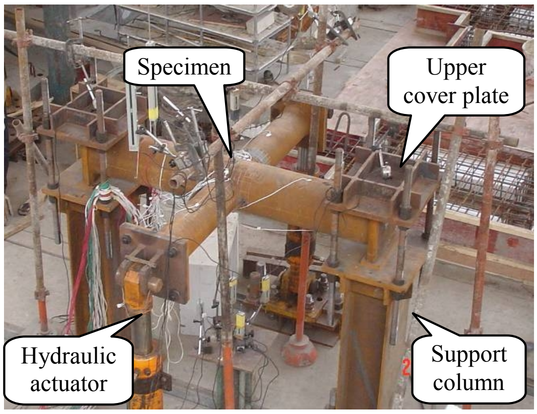

Figure 3. Photo of test setup

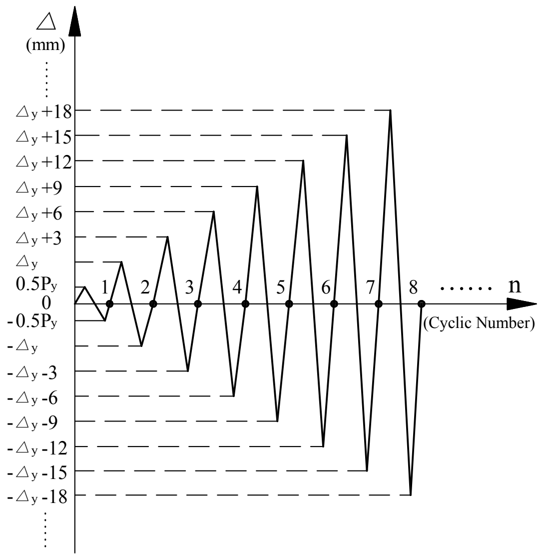

Figure 4. Loading scheme

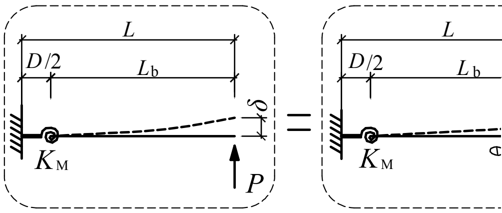

In Equation 1, δ and L_b can be obtained from the test, but it would be difficult to obtain δ_2 from the test. δ_2 can be indirectly obtained by the help of FEA program. Make cantilevered brace model by the solid element, as shown in Figure 7, whose size is exactly the same as specimen and whose end is clipped at the saddle point of chord tube. Make a large displacement static analysis on it, whose material property is from the result of material test.

Figure 5 Model of half specimen

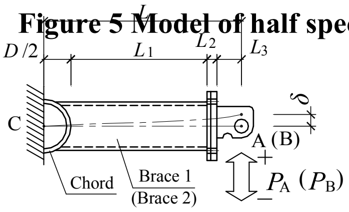

Figure 6. Composition of the

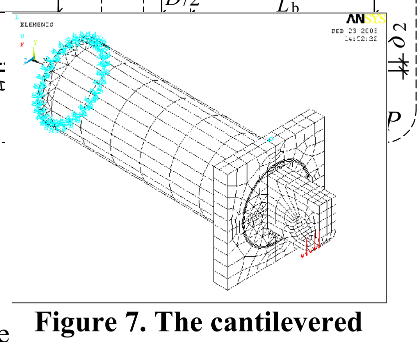

Figure 7. The cantilevered brace FEA model

5. TEST RESULT

5.1 Specimen failure

All specimens were loaded cyclically up to failure, and the process is described in Table 3. Figure 8 shows the specimens after tests.

Table 3. Observation of specimens

Specimen	Failure mode and process
XBH-1 XBH-2	The chord tube wall cracked at the outside of saddle points after the tube wall developed certain plastic deformation. The failure mode is punching of the chord tube wall.
XBH-3	The brace tube wall buckled when the section is plastic, and the chord wall had no failure phenomenon

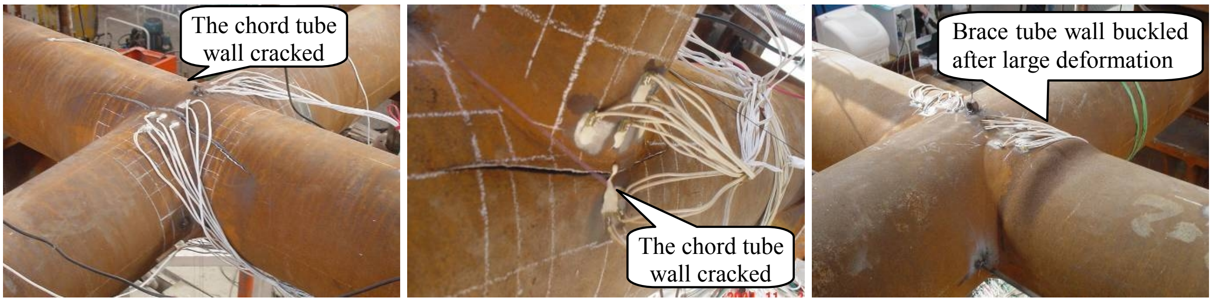

(a) XBH-1 **(b) XBH-2** **(c) XBH-3**

Figure 8. The failure of specimens

5.2 Test curve

5.2.1 Applied load - the brace end displacement (relative to the center) hysteretic curve

Applied load P of the brace end and the brace end displacement δ (relative to center) relationship curves are shown in Figure 9 ~11. In the figures, skeleton curve is given out according to the hysteretic curve. And initial yield load P_y and fully plastic load P_p of brace tube calculated by the equation of elastic-plastic mechanics are noted. In (a), (c), and (e), arrow "A" indicates the point when the specimen was firstly found to failure. From the figures it can be found that the capacities of specimens are all higher than the fully plastic load P_P.

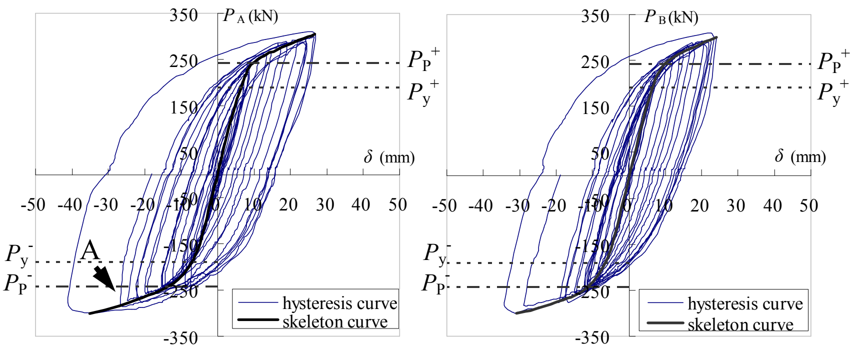

(a) Brace 1 **(b) Brace 2**

Figure 9. Applied load - brace end displacement of XBH-1

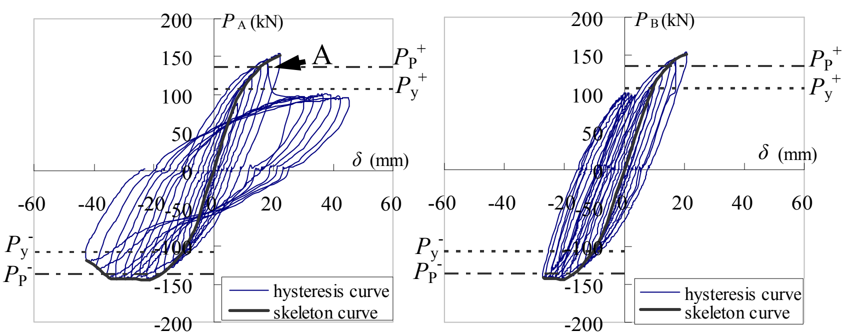

(a) Brace 1 **(b) Brace 2**

Figure 10. Applied load - brace end displacement of XBH-2

5.2.2 The joint moment - joint rotation skeleton curve

The joint Moment M - joint

rotation θ skeleton curve is shown in Figure 10. The joint moment M adopted the value at the crown point, resulting from the applied load P.

From the skeleton curves of the joints, we can evaluate some indicators to assess the performance of the joint. To determine the yield displacement and force, a method recommended by Kurobane, Y. et al [4] is employed. To take the initial stiffness of skeleton curve as K_M, then a line with the slope as $0.779K_M$ is drawn from the origin. The intersection of the line and the skeleton curve gives the yield force and displacement. In this test, the yield force and displacement in tension and compression is listed in Table 4 and Table 7 respectively

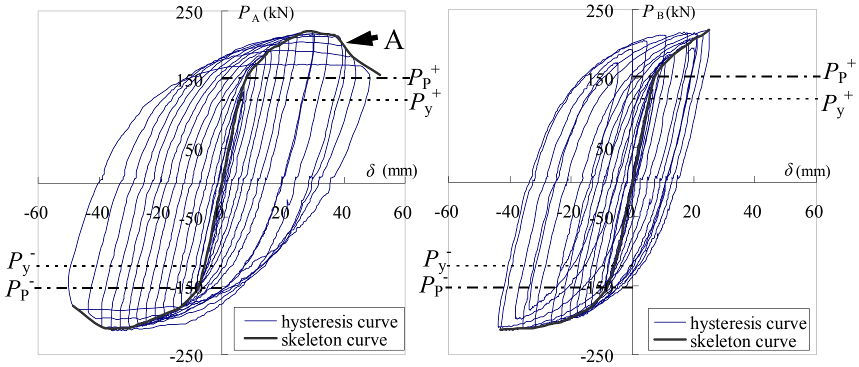

(a) Brace 1 (b) Brace 2

Figure 11. Applied load - brace end displacement of XBH-3

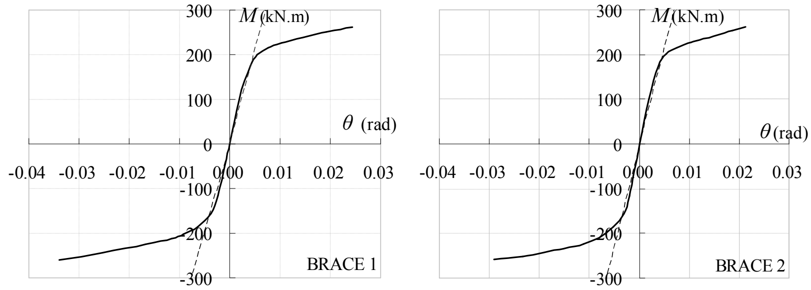

(a) Brace 1 of XBH-1 **(b) Brace 2 of XBH-1**

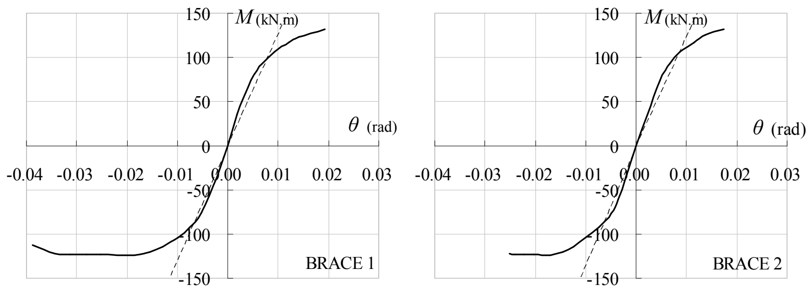

(c) Brace 1 of XBH-2 **(d) Brace 2 of XBH-2**

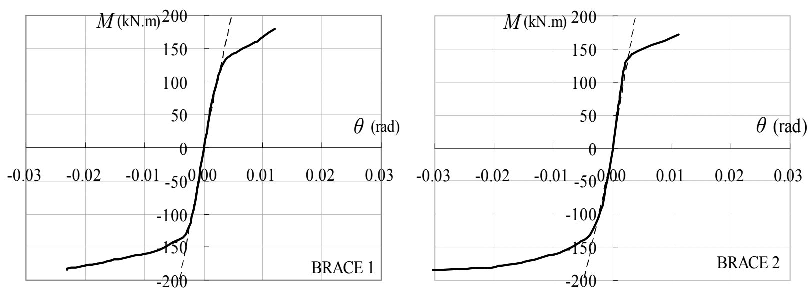

(e) Brace 1 of XBH-3 **(f) Brace 2 of XBH-3**

Figure 12. The Moment M - the joint rotation θ skeleton curve

6. ANALYSIS OF THE RESULT

6.1 Analysis of joint capacity

Joint capacities from the test are listed in the Table 4, in which M_y is obtained according to the method of Kurobane, Y. et al [4] as described in above section, and M_u is the peak value of the joint Moment M - joint rotation θ skeleton curve.

The expected capacities calculated by the equation of codes and elastic-plastic mechanics are listed in the Table 5. M_u^{pjEuro} and M_u^{pjAPI} are capacities calculated by the equation of Eurocode 3 [5] and API-WSD [6] respectively, which are used to indicate the chord tube wall plasticity. M_{ps}^{pj}, calculated by the equation in CIDECT [7], is used to indicate the chord tube wall punching. M_{by} and M_{bp} are initial yield bending capacity (Wf_y) and fully plastic bending capacity (W_pf_y) of brace tube calculated by the equation of elastic-plastic mechanics. Comparison of carrying capacities is listed in Table 6.

In the XHB-1 line of Table 6, the ration M_u/M_{ps}^{sj} is larger than others. And combined with the failure phenomenon, the failure mode of XBH-1 is punching shear. In the XBH-2 line, the ration M_u/M_{ps}^{sj} is appropriately equal with others. And combined with the failure phenomenon, the failure mode of XBH-2 is punching shear. In the XBH-3 line, the ration M_u/M_{bp} is larger than others. And combined with the fracture phenomenon, the failure mode of XBH-3 is buckling of brace tube wall after a large plastic deformation.

From Table 6, we can see that the ultimate carrying capacity of the joints is high, which means that the ultimate capacity is higher than or about equal with the full plastic capacity of brace tube.

Table 4. Carrying capacities from the test (kN-m)

Specimen	M_u^{pjEuro}	M_u^{pjAPI}	M_{ps}^{pj}	M_{by}	M_{bp}
XBH-1	240	249	209	191	242
XBH-2	122	133	131	101	136
XBH-3	258	267	217	121	153

Note: superscript + represents positive loading, while superscript – is negative loading. The values having bold-font are the ultimate capacities of which loading side the fractures were found.

Table 5. Carrying capacities calculated by the equations (kN-m)

Specimen	M_{y1}^+	M_{y1}^-	M_{y2}^+	M_{y2}^-	M_u^+	M_u^-
XBH-1	185	166	188	163	262	**259**
XBH-2	99	89	107	87	**131**	124
XBH-3	118	123	133	113	**189**	185

Table 6. Comparison of Carrying capacities

Specimen	M_u^+/M_y^+	M_u^-/M_y^-	M_u/M_u^{pjEuro}	M_u/M_{ps}^{sj}	M_u/M_{bp}
XBH-1	1.39	1.56	1.08	1.25	1.08
XBH-2	1.22	1.39	1.01	1.0	0.96
XBH-3	1.42	1.50	0.72	0.87	1.23

M_u^{pjEuro} used to calculate the capacity of chord tube wall plasticity is given out by Equation 2. And M_{ps}^{pj} used to calculate the capacity of chord tube wall punching is given out by Equation 3.

$$M_u^{pjEuro} = \frac{2.7}{1-0.81\beta}\frac{1}{\sin\theta}(dT^2 f_y) \tag{2}$$

$$M_{ps}^{pj} = (\frac{3+\sin\theta}{4\sin^2\theta})d^2Tf_v = (\frac{3+\sin\theta}{4\sin^2\theta})\frac{1}{\sqrt{3}}\beta\gamma(dT^2 f_y) \tag{3}$$

By Comparing Equation 2 with Equation 3, a conclusion can be drawn that when γ gets smaller while other parameters keep the same, the failure mode of joint tends to be punching, instead of chord tube wall plasticizing. The ratio γ of XBH-1 and XBH-2 is smaller, so they tend to be punching.

6.2 Analysis of joint ductility

Ductility is an important indicator to assess seismic resistance. The ductility ratio is defined as $\mu = \theta_u/\theta_y$, where θ_u is the ultimate rotation and θ_y is the yield rotation. The ductility ratio in the tension is defined as $\mu^+=\theta_u^+/\theta_y^+$ and in the compression as $\mu^-=\theta_u^-/\theta_y^-$. From the curve given in Figure 10, the ductility ratios in tension and in compression are listed in Table 7 respectively.

From the table, the ultimate rotations and ductility ratios of XBH-1 are larger than 0.02 and 4 respectively, so it can be considered excellent in ductility. The ultimate rotations and ductility ratios of XBH-2 are smaller than 0.02 and 3 respectively, so it can be considered poor in ductility. Since the test did not reach the fracture of chord tube of XBH-3, the values do not represent the realistic

Table 7. The ductility ratio of joints under bending load

Specimen (XBH-*)		θ_y^+	θ_u^+	θ_y^-	θ_u^-	μ^+	μ^-
1	Brace1	0.0045	0.024	0.0044	0.034	5.4	7.8
	Brace 2	0.0045	0.021	0.0037	0.029	4.7	7.8
2	Brace 1	0.0079	0.019	0.0069	0.019	2.4	2.8
	Brace 2	0.0087	0.017	0.0065	0.017	2.0	2.6
3	Brace 1	0.0028	>0.012	0.0025	>0.023	>4.3	>9.0
	Brace 2	0.0026	>0.011	0.0027	>0.032	>4.3	>11.7

ductility of the joint.

The difference of geometry between XBH-1 and XBH-2 is that the ration β of XBH-1 is larger than that of XBH-2. So it can be considered that when the ration γ is large, the joint whose value of β is larger has better ductility. The reason may be that when the value of β is larger, the chord wall between two saddle points at the same side of specimen plane would be more easy to produce large plastic deformation, and the stress concentration factor outside the line of intersection is more reduced, which means that it is more difficult to fracture for the joint.

7. CONCLUSIONS

The failure loads of three specimens are all higher than or approximately equal with the fully plastic capacity of brace tube. So the joint of proper geometrical parameters and qualified welds can acquire a high ultimate carrying capacity.

By the analysis of carrying capacities and failure modes, a conclusion can be drawn that when γ gets smaller while other parameters keep the same, the failure mode of joint tends to be punching of chord tube wall, instead of chord tube wall plasticizing.

By the analysis of ductility and energy dissipation, it can be considered that when the ration γ is large, the joint whose value of β is larger behave excellent in deformability and energy-dissipation, the other worse in this regard.

ACKNOWLEDGEMENTS

Financial support (Grant No. 50578117) from the National Natural Science Foundation of China for this project is greatly appreciated.

REFERENCES

1. Kurobane, Y., "Static behavior and earthquake resistance design of welded structures," *Mechanics and Design of Tubular Structures*, edited by Jarnai, K & Farkas, J. 53-116, 1998
2. Wang, W. & Chen, Y. Y., "Hysteretic behavior of the tubular joints under cyclic loading," *Journal of construction Steel Research*, Vol.63, 2007, pp. 1384-1395.
3. Chen, Y. Y. & Zhao, X. Z., "Experimental study on hysteretic behavior of CHS overlap K-joints and gap KK-joint," *Proc. of 5th International Conference on Advances in Steel Structures*, Vol.II, 207-217, Singapore, 2007.
4. Kurobane, Y., Makino, Y. and Ochi, K., "Ultimate Resistance of Unstiffened Tubular Joints," *Journal of structural Engineering*, Vol. 110, No. 2, February, 1984, pp. 385-400.
5. CEN, "Eurocode 3: Design of steel structures, part 1.1 - General Rules and Rules for Buildings," *DD ENV 1993-1-1*, European Committee for standadization, London, UK, 1992.
6. American Petroleum Institute, "Recommended practice for planning, designing and constructing fixed offshore platforms - working stress design," *API RP2A-WSD, 20th edition*, 1993.
7. Wardenier, J., Kurobane, Y., Packer, J. A., Dutta, D., and Yoemans, N. "Design guide for circular hollow section (CHS) joints under predominantly static loading." *CIDEC series: Construction with hollow steel sections,* TÜV-Verlag Gmbh, Köln, Germany 1991.